LB-107

Repurposing endogenous immune pathways to improve chimeric antigen receptor T-cells potency

Mohit Sachdeva[1], Brian Busser[1], Sonal Temburni[1], Alexandre Juillerat[1], Laurent Poirot[2], Philippe Duchateau[2] and Julien Valton[1]

[1] Cellectis, Inc., 430E, 29th street, New York, NY 10016, USA; [2] Cellectis, 8 rue de la Croix Jarry, 75013 Paris

#1 Abstract

CAR T-cell therapies hold great promise for treating a range of liquid malignancies but are however challenged to access and eradicate solid tumors. To overcome this hurdle, CAR T-cell were engineered to secrete different cytokines known to improve T-cell antitumor activity, prevent T-cell anergy and reduce activation induced cell death. While cytokine-expressing CAR T-cell were shown to be highly active against solid tumor in in vivo models, they have also led to toxicity associated with the systemic release of cytokine. Therefore, new engineering strategies enabling the fine tuning of cytokine secretion by CAR T-cell are warranted.

We sought to explore one of these engineering strategies by integrating an IL-12 chimeric heterodimer expression cassette under the control of the endogenous promoters regulating PD1 or CD25. Because both genes are known to be activated upon tumor engagement by CAR T-cells, they could be repurposed to secrete cytokine only in the vicinity of a given tumor. This approach would reduce the potential side effects induced by their systemic secretion while maintaining their capacity to improve antitumor activity.

By combining TALEN® technology with AAV6 repair vectors delivering the CAR to the TRAC locus and the IL-12 to the CD25 or PD1 loci, we have engineered CAR and IL-12 expressions under the respective control of TCR and CD25 or PD1 regulatory elements. This double targeted insertion led to the disruption of PD1 and TRAC genes, to the non disruptive modification of CD25 gene, to the expression of a CAR along with the conditional secretion of IL-12 in the media. Such secretion was found to be transient, dependent on tumor engagement and to follow the regulation patterns of CD25 or PD1 genes, commonly observed upon T-cell activation. In addition, it was also found to enhance the antitumor activity and the proliferative capacities of CAR T-cells.

#2 Repurposing CAR T-cells immune pathways to tailor secretion of IL-12 upon tumor engagement

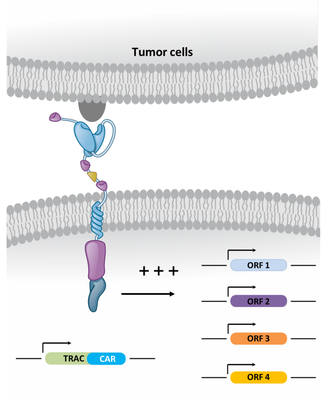

A whole array of genes could be repurposed by TALEN®-mediated targeted insertion of IL-12.

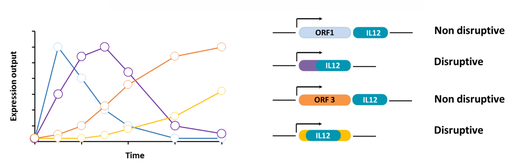

#3 Repurposing TCR, CD25 and PD1 genes expression

Matrix design for IL-12 insertion at the CD25 and PD1 loci and of anti-CD22 CubiCAR insertion at the TRAC locus

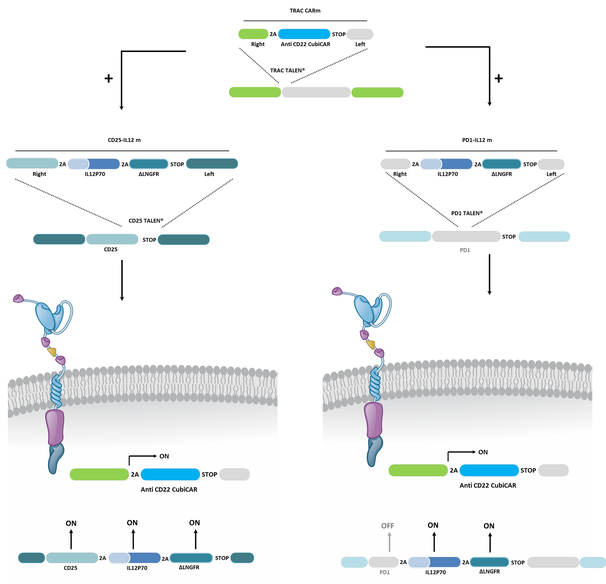

#4 Efficient TALEN®-mediated targeted insertion of CAR at the TRAC locus

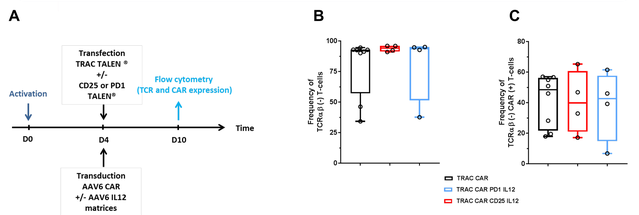

Figure 1. (**A**) Protocol used to perform double targeted insertions of the CARm at the TRAC locus and CD25 IL-12m and PD1 IL-12m at their respective CD25 or PD1 loci. T-cells were activated using CD3/CD28 Dynabeads, cultivated for 4 days before being transfected and transduced by TRAC TALEN® and the CARm alone (TRAC CAR) or in the presence of CD25 or PD1 TALEN® and CD25 IL-12m and PD1 IL-12m (TRAC CAR CD25 IL12 or TRAC CAR PD1 IL12). T-cell were recovered 6 days post transfection/transduction, stained by CD3 and CAR specific antibodies (QBEND10) and analyzed by flow cytometry. (**B**) and (**C**) Frequency of TCRα/β (-) T-cells and frequency of CAR expression within TCRα/β (-) T-cells obtained in the three different conditions.

#5 TALEN®-mediated insertion of IL-12 matrices disrupts PD1 and spares CD25 expressions

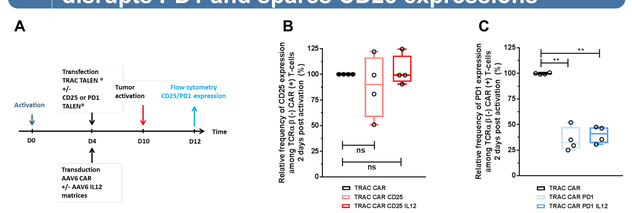

Figure 2. (**A**) Protocol used to determine the impact of double targeted insertions (CARm at the TRAC locus and CD25 IL-12m or PD1 IL-12m) on the expression of CD25 and PD1. Following the protocol described in figure 1, 1E^6 CAR T-cells were activated by CD22 expressing tumor cells at E/T ratio of 1, cultivated for 2 days before being analyze by flow cytometry for surface expression of CD25 and PD1. Two control groups, consisting of CAR TRAC T-cell edited by CD25 or PD1 TALEN® in the absence of their corresponding IL-12 matrices were performed. (**B**) and (**C**) Frequency of CD25 and PD1 positive cells among TCRα/β (-) CAR (+) T-cells obtained in the different conditions One way ANOVA was used for statistical analysis (**, p-value<0.001).

#6 Converting CAR T-cell/tumor engagement into IL-12 secretion

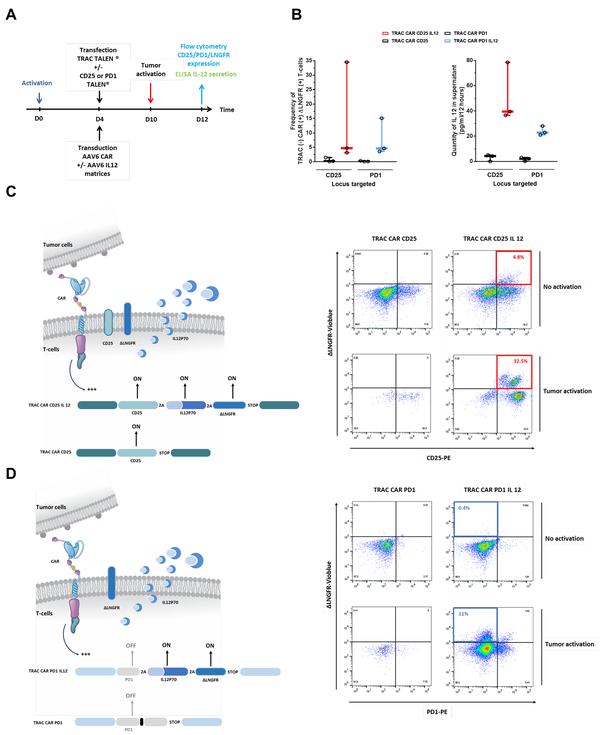

Figure 3. (**A**) Protocol used to characterize the expression of CD25, PD1 and LNGFR, and assess the concomitant secretion of IL-12 upon tumor engagement. (**B, left panel**) Frequency of LNGFR positive cells among TCRα/β (-) CAR (+) T-cells obtained in the different conditions. (**B, right panel**) Quantity of IL-12 detected in the media after 12 hours of CAR T-cell incubation with tumor cells at a E:T ratio of 1:1. (**C**) and (**D**) Representative flow cytometry plots illustrating concomitant expression of CD25/LNGFR and PD1/LNGFR by TCRα/β (-) CAR (+) T-cells respectively.

#7 Il-12 secretion is tightly regulated and follows CD25 and PD1 expression patterns

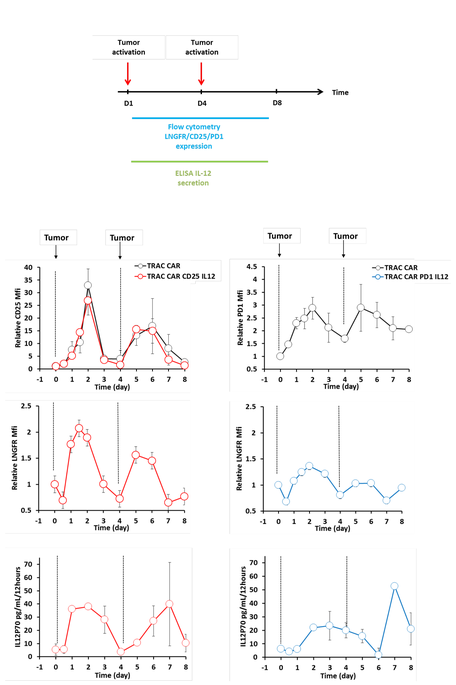

Figure 4. (**A**) Protocol used to characterize the regulation of CD25, PD1 and LNGFR expression and IL-12 secretion as a function of time. 1E^6 CAR T-cells were activated by CD22 expressing tumor cells at D1 and D4 using an E/T ratio of 1 and analyze by flow cytometry at different time points for surface expression of CD25, PD1 and LNGFR and determine the amount of IL-12 released in the supernatant. Two control groups, consisting in CAR TRAC T-cell edited by CD25 or PD1 TALEN® in the absence of their corresponding IL-12 matrices were performed. (**B, upper panel**) Evolution of relative CD25 or PD1 MFIs among TCRα/β (-) CAR (+) T-cells. (**B, middle panel**) Evolution of the relative ΔLNGFR MFI among TCRα/β (-) CAR (+) T-cell. (**B, bottom panel**) Evolution of IL-12 secretion expressed as pg/mL of supernatant recovered every 12 hours.

#8 Conditional secretion of IL-12 increases the antitumor activity of CAR T-cells *in vitro*

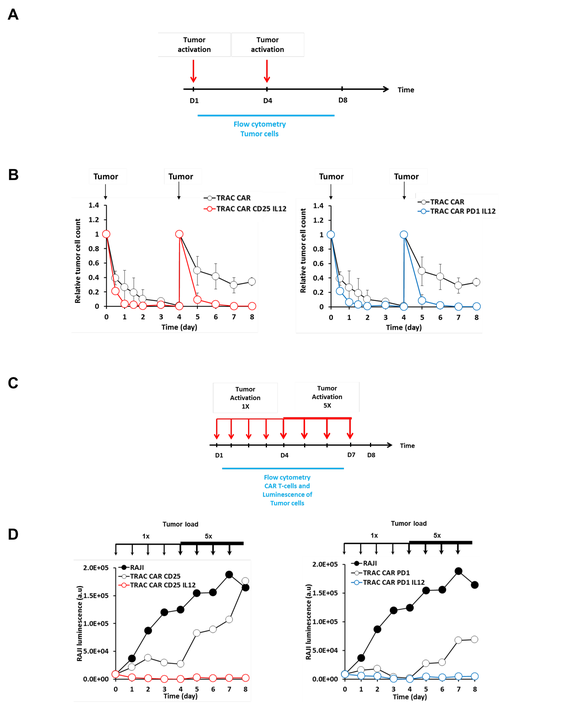

Figure 5. (**A**) Protocol used to characterize the kinetic of tumor cell depletion by CAR T-cells. 1E^6 CAR T-cells were mixed with fresh CD22 expressing tumor cells (Raji-luciferase) at D1 and D4 using an E/T ratio of 1. Cell mixture was analyzed by flow cytometry to determine the depletion of tumor cells as a function of time. The remaining number of tumor cell obtained after each time point were determined and normalized to the initial number of tumor cell added. (**B**) Kinetic of tumor cell depletion by TRAC CAR T-cell edited at the CD25 locus with or without IL-12m (**left**) and by TRAC CAR T-cells edited at the PD1 locus with or without IL-12m (**right**). (**C**) Protocol used to characterize long cytolytic activity of CAR T-cells. CAR T-cell were challenged by daily addition of Raji-luciferase (0.2E^6 cells/ml/well in 1 mL total volume) for 4 days and eventually challenged by daily addition of 5 time more CD22 expressing tumor cells from day 5 to day 8. Every day, cell mixtures were centrifuged and resuspended into fresh media containing fresh Raji-luciferase cells. Antitumor activity of CAR T-cell was monitored everyday by measuring the luminescence signal emitted by the remaining Raji-luciferase cells. (**D**) Evolution of luciferase signal as function of time

#9 Regioselective and tumor dependent secretion of IL-12 by CAR T-cells *in vivo*

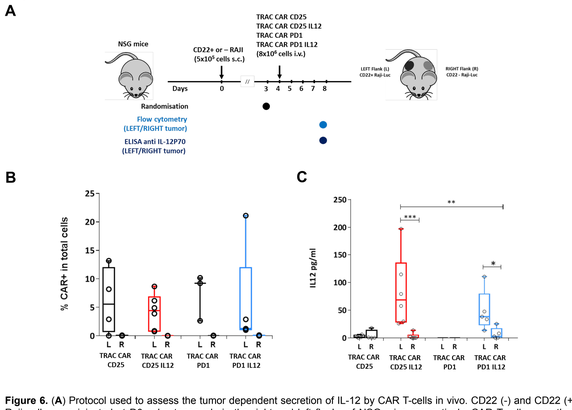

Figure 6. (**A**) Protocol used to assess the tumor dependent secretion of IL-12 by CAR T-cells in vivo. CD22 (-) and CD22 (+) Raji cells were injected at D0 subcutaneously in the right and left flanks of NSG mice respectively. CAR T-cells were then injected i.v at D4 and the tumor nodules were recovered from the right and left flanks at D8 for analysis by flow cytometry and by IL-12 specific ELISA assay. (**B**) Frequency of CAR (+) T-cells detected in the right and left flanks of NSG mice. (**C**) Quantity of IL-12 detected in the right and left flanks of NSG mice. One-way ANOVA was performed for statistical analysis of the data. **, p-value<0.001; *, p-value<0.05.

#10 Conclusions

Here we combined the TALEN® technology with AAV6 repair vectors to engineered CAR and IL-12 expressions under the respective control of TCR and CD25 or PD1 regulatory elements. This engineering strategy spared CD25 expression, disrupted PD1 and TRAC genes, elicited the expression of a CAR and the conditional secretion of IL-12 in the media. IL-12 secretion was found to be transient, regioselective, dependent on tumor engagement and to follow the regulation patterns of CD25 or PD1 genes. It was also found to markedly enhance the short and long term antitumor activity of CAR T-cells.

This work provide a proof of concept that T-cell immune pathways could be engineered to efficiently translate a given input (CAR/tumor engagement) into a tailored output (IL-12 secretion). This engineering strategy could be applied to repurpose a myriad of different other genes to deliver therapeutically relevant factors in a conditional and tightly regulated manner.

Pre-clinical Efficacy of Allogeneic Anti-CD123 CAR T-Cells for the Therapy of Blastic Plasmacytoid Dendritic Cell Neoplasm (BPDCN)

#2560

Tianyu Cai[1], Kathryn L Black[2], Ammar Naqvi[2], Roman Galetto[3], Agnès Gouble[3], Julianne Smith[4], Antonio Cavazos[1], Lina Han[1], Qi Zhang[1], Vinitha Kuruvilla[1], Sergej Konoplev[1], Sattva S. Neelapu[1], Andrew A. Lane[5], Monica Guzman[6], Hagop Kantarjian[1], Andrei Thomas-Tikhonenko[2], Naveen Pemmaraju[1], Marina Konopleva[1]

[1]UT MD Anderson Cancer Center, Houston, TX; [2]The Children's Hospital of Philadelphia, Philadelphia, PA; [3]Cellectis SA, Paris, France; [4]Cellectis Inc, New York, NY; [5]Dana-Farber Cancer Institute, Boston, MA; [6]Weill Cornell Medical College, New York, NY

Abstract

Blastic plasmacytoid dendritic cell neoplasm (BPDCN) is a rare, aggressive hematologic malignancy with historically poor outcomes and no established standard of care. Nearly 100% of patients with BPDCN overexpress CD123, and targeting CD123 emerged as an attractive therapeutic approach given its differential expression on BPDCN cell surface.

UCART123 product (Cellectis) uses genetically modified allogeneic T-cells (derived from healthy donors, so-called "off the shelf") containing an anti-CD123 CAR and a RQR8 depletion ligand that confers susceptibility to rituximab. The expression of the T-cell receptor (TCR) is abrogated through the inactivation of the *TCRα* gene, using Cellectis' TALEN® gene-editing technology.

We have previously reported the selective *in vitro* anti-tumor activity of UCART123 cells against CD123 (+) primary BPDCN samples using cytotoxicity assays, T-cell degranulation assay and the secretion of IFNγ and other cytokines (IL2, IL5, IL6, IL-13 and TNF-α) by UCART123 cells when cultured in the presence of BPDCN cells *(Tianyu Cai, 2017 ASH)*. Furthermore, UCART123 had minimum toxicity against normal bone marrow cells.

To evaluate in vivo anti-tumor activity of UCART123 cells, we established two patient-derived xenografts (PDX1-2) from patients with relapsed BPDCN in NSG-SGM3 mice. In PDX-1 model, all mice in vehicle-treated group died by D53, with high tumor burden in peripheral blood, spleen and bone marrow. Three out of 9 (33%) mice treated with 3×10^6 UCART123 and six out of 9 (67%) mice treated with 10×10^6 UCART123 were alive and disease-free at the end of the study (D299).

In PDX-2 model, while UCART123 similarly extended survival of the mice (D104-241), relapses occurred in all treatment cohorts at D90-155. Flow cytometric analysis showed that all of the relapses in 10×10^6 UCART123 group were associated with emergence of CD123 (-) BPDCN clones (95-96% CD123 (-)). To understand the molecular basis for loss of CD123 surface expression, we isolated RNA from two CD123 positive samples from vehicle group and one CD123 negative samples from 1×10^6 UCART123 group. RT-PCR and RNA-seq detected the presence of full-length transcripts containing exons 1-12 in both CD123 (+) samples. In the CD123 (-) samples, CD123 transcripts were completely absent, along with loss of transcripts of neighboring genes.

In summary, UCART123 therapy results in BPDCN eradication and long-term disease-free survival in primary BPDCN PDX models. However, loss of CD123 through diverse genetic mechanisms could lead to escape from UCART123 therapy and cause relapses. A phase I trial of UCART123 in BPDCN is opened for enrollment (NCT03203369).

Cytotoxic activity of UCART123 cells against primary BPDCN cells in vitro

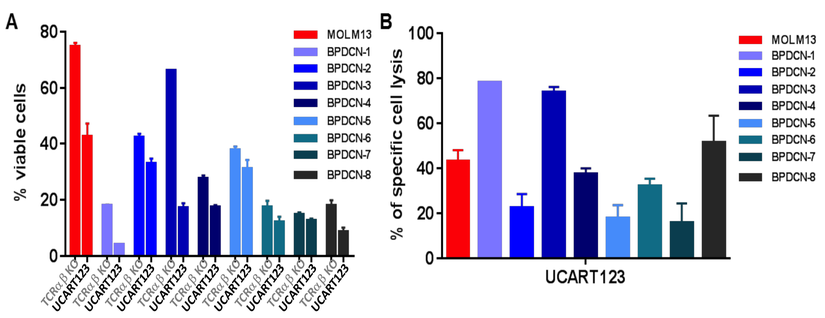

Figure 1. Cytotoxic activity of UCART123 cells against primary BPDCN cells in vitro. Panel A: Viability of the different CD123 (+) MOLM13 cell line or patient samples upon 16h co-culture with either UCART123 cells or non-transduced TCRαβ-deficient T-cells (TCRαβ KO). Each point represents the data obtained from triplicate experiments and the mean+/- SD value is shown. Panel B shows the specific cytotoxic activity against target cells for each of the CD123 (+) cell line or patient sample upon 16h co-culture with either UCART123 cells or TCRαβ KO T-cells. Frozen UCART123 and TCRαβ KO T-cells were thawed and immediately co-cultured with target cells.

IFNγ release assay

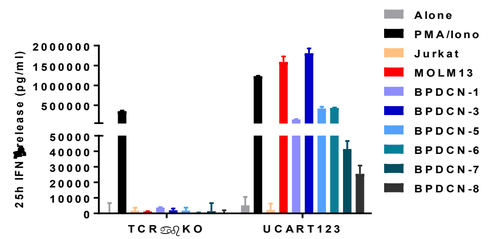

Figure 2. IFNγ release assay upon co-culture of UCART123 cells, or TCRαβ KO T-cells with CD123(-) or CD123(+) cells. IFNγ was examined using BioLegend's LEGENDplex™ assay. PMA/Ionomycin was used as a positive control.

UCART123 therapy results in BPDCN eradication and long-term disease-free survival in a primary BPDCN PDX model

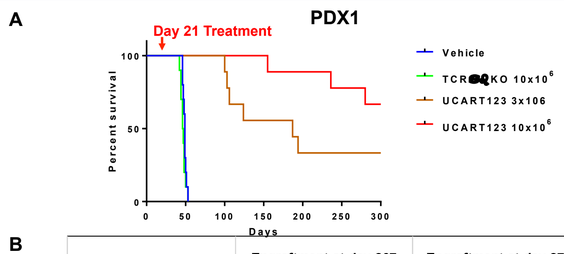

B

	Engraftment at day 267 (CD123+ CD56+)	Engraftment at day 279 (CD123+ CD56+)
UCART123 3×10^6 groups	0.1%	0.0%
	0.0%	0.0%
	0.2%	0.0%
UCART123 10×10^6 groups	0.0%	0.1%
	0.1%	0.0%
	0.2%	0.0%
	0.1%	0.0%
	0.0%	0.0%
	0.2%	0.0%
	0.1%	0.0%

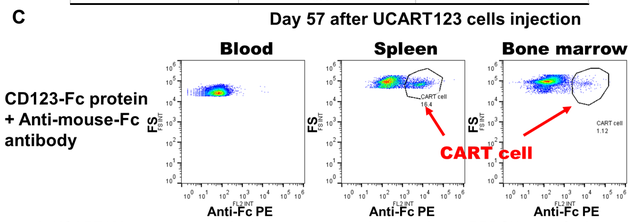

Figure 3. UCART123 treatment results in long-term survival in primary BPDCN engrafted xenograft. NSGS mice were injected with a primary BPDCN sample BPDCN-1 (68.4% CD123 (+) cells, 2×10^6 tail veil injection at day 0). Engraftment was confirmed by retro-orbital bleeding after 21 days, and then mice were treated with a single injection of vehicle, 10×10^6 TCRαβ KO T-cells, 3×10^6 UCART123 or 10×10^6 UCART123 cells. (A) Treatment with UCART123 resulted in significant survival extension. (B). UCART123 reduce or eliminate circulating tumor (BPDCN) burden. Circulating tumor burden measured by flow cytometry in peripheral blood samples from mice collected on the indicated days (post tumor injection), using 9F5 monoclonal Anti-CD123-PE antibody (555644, BD Pharmingen) and B159 monoclonal Anti-CD56-APC antibody (555518, BD Pharmingen) gating on viable cells (DAPI(-)).

Loss of CD123 leads to escape from UCART123 therapy and causes relapses

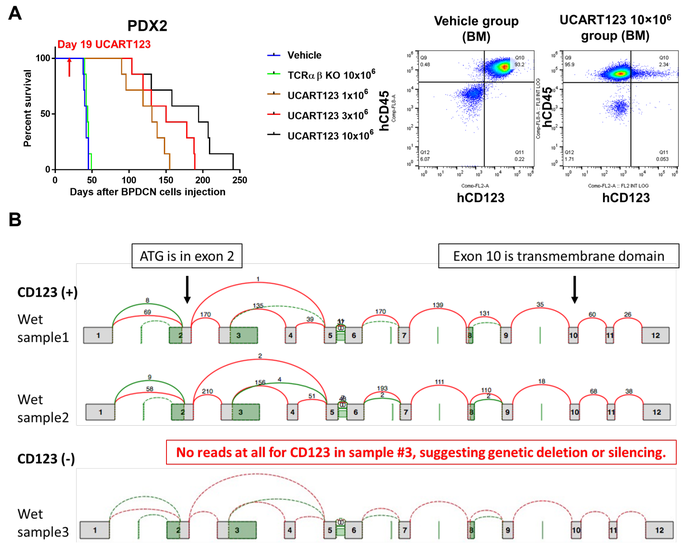

Figure 4. PDX3 model. NSG-S mice injected with a primary BPDCN3 sample were randomized on Day 19 upon documented engraftment (13.9% and 33.8% engraftment in BM from 2 randomly selected mice) to receive vehicle; 10×10^6 TCRαβ KO control T cells; 1×10^6 UCART123 cells, 3×10^6 UCART123 cells or 10×10^6 UCART123 cells. (A) Left, survival of mice in different therapy groups was estimated using Kaplan-Myer method. Right, expression of CD123 on tumor cells isolated from bone marrow of diseased vehicle-treated or UCART123-treated mice upon sacrifice from disease, using anti-CD123-PE antibody, anti-CD45-APC-Cy7 antibody and gating on viable cells (DAPI(-)). Tumor cells from UCART123-treated mice were largely CD123 (-) but remained CD56(+). (B) RNA was isolated from two CD123 (+) samples from vehicle group and a CD123 (-) samples from 1×10^6 UCART123 group. RT-PCR and RNA-seq detected the presence of full-length transcripts containing exons 1-12 in both CD123 (+) samples. In the CD123 (-) samples, CD123 transcripts were completely absent, along with loss of transcripts of neighboring genes.

Conclusions

- UCART123 therapy results in BPDCN eradication and long-term disease-free survival in primary BPDCN PDX models.
- In some cases, relapses seem to occur with loss of CD123 through diverse genetic mechanisms.

Acknowledgement

- UCART123 research grade cells and research funding were provided by Cellectis SA, France.

Prediction of immunotherapy outcome by multimodal assessment of minimal residual disease and persistence of allogeneic anti-CD123 CAR T-cells (UCART123) in pre-clinical models of acute myeloid leukemia

Mayumi Sugita, MD[1]*, Nuria Mencia-Trinchant, PhD[1], Nathan Ewing-Crystal[1], Gabrielle Suppa[1], Roman Galetto, PhD[2], Agnes Gouble, PhD[2], Julianne Smith, PhD[3], Gail J. Roboz, MD[1], Duane C. Hassane, PhD[1], and Monica L. Guzman, PhD[1]

[1]Weill Cornell Medicine, New York, NY; [2]Cellectis SA, Paris, France; [3]Cellectis Inc, New York, NY

Abstract

Acute myeloid leukemia (AML) is a fatal disease. The promise of autologous T-cells expressing chimeric antigen receptors (CARs) in targeting B-cell malignancies has encouraged extension of this approach to AML. However, clinical guidance regarding infusion and re-infusion regimens for CAR-T technology is unclear for any cancer including AML. Given that studies demonstrate clear benefit for minimal residual disease (MRD) assessment in predicting relapse for AML, we thus sought to ascertain whether simultaneous molecular assessment of MRD markers and CAR-T-specific markers could inform decisions around CAR-T dosing and re-infusion. We tested this approach using patient-derived xenograft (PDX) models with allogeneic anti-CD123 CAR-T cells (UCART123). UCART123 are genetically modified allogeneic T-cells expressing an anti-CD123 CAR. These cells lack expression of the T-cell receptor (TCRαβKO), in order to minimize graft vs. host disease (GvHD).

PDX were established using prognostically adverse AML (FLT3-ITD+NPM1+) and treated with 1x10^6 or 2.5x10^6 UCART123. The median overall survival (OS) of control mice injected with saline or CAR-T negative (TCRαβKO) T-cells succumbed to disease was 124.5 and 126 days, respectively. In contrast, UCART123 groups survived >180 days (hazard ratio 0.08, p=0.003). Clonal dynamics between disease and CAR-T were simultaneously monitored post-infusion by quantifying mutated NPM1 and CAR-T genetic markers, respectively, using digital droplet PCR (ddPCR). We found that ddPCR monitoring was more sensitive than multiparameter flow cytometry (MFC) at detecting MRD and persistence of UCART123. Using ddPCR, leukemia and UCART123 cells were detected when human cells were not evaluable using MFC in peripheral blood (PB). Mice with persistent UCART123 remained disease-free. Importantly, when mutated NPM1 levels became elevated with simultaneous loss of UCART123, relapse was evident by MFC in PB in subsequent time-points (2 out 20 mice, all at 1x10^6 dose, ~180 days) re-infusion of UCART123 cells resulted in effective elimination of AML.

Taken together, we have demonstrated that simultaneous monitoring of disease and UCART123 cells provides valuable insight into the kinetics and effectiveness of UCART123 cells. Currently, we have implemented the ddPCR assay in the phase I clinical trial of UCART123 in AML allowing to simultaneously detect UCART123 cells and blasts in peripheral blood of NPM1 mutant AML patients.

Introduction

Allogeneic approach to targeting CD123

CD123, Interleukin-3 receptor alpha chain, is highly expressed in AML stem cells aberrantly and is a potential target to eliminate leukemia stem cells in AML. One of the key barriers to the adoptive transfer of 3rd party CAR T-cells can be overcome via the application of TALEN® gene editing technology: inactivation of the TCRα gene would lead to TCRαβ complex disruption at the T-cell surface, and allow the use of any donors' T-cells

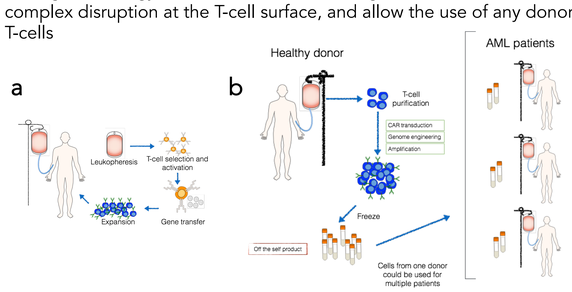

Figure 1. Chimeric antigen receptors (CARs) T cell approaches.
(a) Autologous T-cell therapy design. (b) Allogeneic T-cell approach.

Methodology

Patient-derived xenotransplants (PDX) were generated to test in vivo activity of UCART123

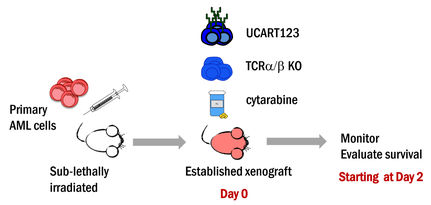

Figure 2. Outline of the in vivo experiment.
A half million of primary AML cells that carries FLT3-ITD and NPM1 mutations were injected into sub-lethally irradiated NSG mice. After conforming engraftment on week 4 post-injection of AML cells, PDX mice were treated with 1x10^6 UCART123 x 1 dose, 2.5 x10^6 UCART123 x 1 dose, 2.5 x10^6 TCRα/β KO x 1 dose, Ara-C 60mg/kg/dose x 5 days or saline as control.

Tracking of leukemia and UCART123 in blood with Flow Cytometry and ddPCR

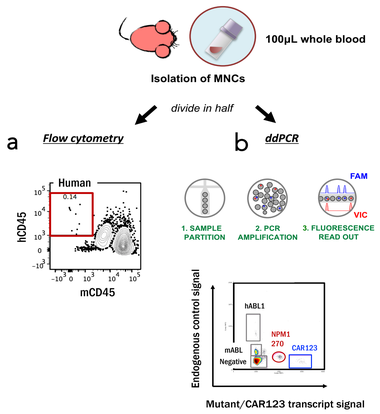

Figure 3. PB samples were monitored by both MFC and ddPCR.

Schema illustrating the approach to simultaneously evaluate UCART123 cells and AML cells by ddPCR and MFC. Briefly, AML cells and UCART123 in PB were evaluated on day 2, day 12, day 21 and day 28, then every 2-3 weeks until mice are dead or be sacrificed due to sickness. (a) AML cells were defined as mouse (m) CD45-/human (h) CD45+/CD33+/CD5- and UCART123 cells were defined as mCD45-/hCD45+/CD33-/CD5+/TCRα/β-. Flow cytometric data was acquired on the LSRFortessa (BD Biosciences) and analyzed with Flowjo (FLOWJO, LLC). (b) Ten million droplets were generated from cDNA samples (step1) and single molecule in droplets are amplified by PCR reaction (step 2) followed by counting the absolute number of fluorescent droplets (step 3). Step 1 and step 3 were performed and analyzed with RainDrop (Source and Sense) and RainDrop Analyst II software (*RainDance Technologies/Bio-Rad Technologies*).

Results

UCART123 significantly decreases tumor burden and improves overall survival

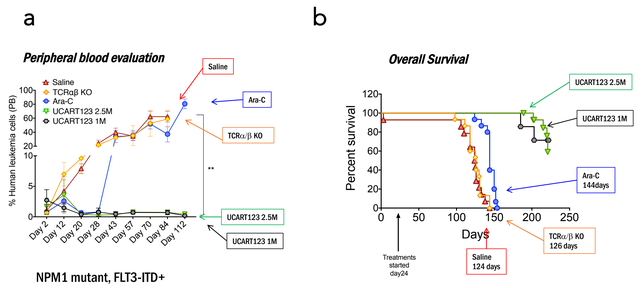

Figure 4. UCART123 cells cleared leukemia cells by day 28 to undetectable level by MFC and led significant longer survival.
(a) Human leukemia burden was tracked by MFC. Conventional treatment, Ara-C, temporarily reduced tumor burden followed by progression of disease as well as control groups that were treated with saline or CAR negative T cells (TCRαβ KO). (b) Groups treated with UCART123 survived longer significantly than control, Ara-C and TCRαβ KO groups.

Persistent UCART123 correlated to longer remission

UCART123 cells and leukemia cells in PB were monitored by tracking CAR123 and NPM1 mutant transcripts by ddPCR. Dramatic swaying of UCART123 and leukemia cells were observed in various patterns individually.

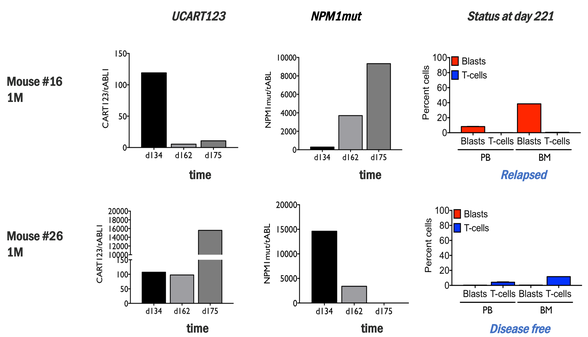

Figure 5. Early detection of leukemia and sustained UCART123 cells by ddPCR predicted the outcome.
(Top rows) early detection of leukemia on day 162 in mouse #16 progressed along with loss of UCART123 cells. (Bottom rows) sustaining UCART123 cells were detected on day 134 and day 162 in mouse #26. Leukemia was cleared away followed by proliferation of UCART123 cells over time and remission was maintained.

UCART123 grants sustained remission

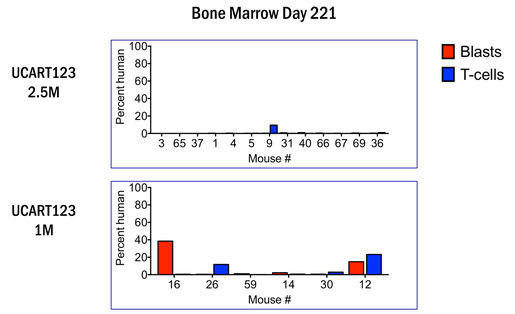

Figure 6. Disease status and persistence of UCART123 in BM at the end of study.

Disease status and persistency of UCART123 was evaluated in BM at the end of study by MFC and ddPCR. (Top) all mice treated with 2.5x10^6 cells of UCART123 remained disease free. (Bottom) In group treated with 1x10^6 cells of UCART123, 3 out of 6 mice had carried leukemia and 3 out of 6 mice were disease-free. This suggests that the higher dose contributes higher rate of long remission.

Conclusion

- UCART123 treatment significantly prolonged overall survival in AML PDX model.
- UCART123 treatment achieved longer disease-free status in a dose-dependent manner.
- Simultaneous monitoring of disease and UCART123 provides valuable insight into the kinetics and effectiveness of UCART123 cells.
- The ddPCR enables early detection of NPM1 mutant AML and UCART123 cells circulating in peripheral blood by using a small amount of sample.

References

1. M. Beurdeley & G.H. Silva: Compact designer TALENs for efficient genome engineering. Nat Commun 2013, 4: 1762.
2. C.T. Jordan, M.L. Guzman & G.L. Phillips et al. : The interleukin-3 receptor alpha chain is a unique marker for human acute myelogenous leukemia stem cells. Leukemia 2000, 14: 1777-1784.
3. N. Mencia-Trinchant, M.L. Guzman, G.J. Roboz & D. C. Hassane: Minimal Residual Disease Monitoring of Acute Myeloid Leukemia by Massively Multiplex Digital PCR in Patients with *NPM1* Mutations. J of Molecular Diagnostics 2017, 19: 537-548.
4. N.M. Cruz, D.C. Hassane & M.L. Guzman: Minimal residua disease in acute myeloid leukemia. Int J Lab Hematol 2017, 39: 53-60.

Disclosures and conflicts of interest

This work is funded by Cellectis Inc.
JS is an employee of Cellectis Inc. RD and AG are employees of Cellectis SA.